Available online at www.sciencedirect.com
SCIENCE DIRECT®
Journal of Solid State Chemistry 177 (2004) 3333–3338
JOURNAL OF SOLID STATE CHEMISTRY
http://elsevier.com/locate/jssc

Photoluminescent multilayer film based on polyoxometalate and tris(2,2-bipyridine)ruthenium

Huiyuan Ma,[a,b] Jun Peng,[a,*] Yanhui Chen,[a] Yuhua Feng,[a] and Enbo Wang[a]

[a] *Faculty of Chemistry, Northeast Normal University, Changchun, 130024, China*
[b] *Faculty of Physics and Chemistry, Harbin Normal University, Harbin 150080, China*

Received 25 March 2004; received in revised form 27 May 2004; accepted 31 May 2004

Available online 20 July 2004

Abstract

A photoluminescent multilayer film based on Keggin-type polyoxometalate $PMo_{12}O_{40}^{3-}$ (PMo_{12}) and transition metal complex tris(2,2-bipyridine) ruthenium $[Ru(bpy)_3]^{2+}$ (Ru(bpy)) was prepared by using layer-by-layer assembly(LBL). The formation of multilayer film was monitored by ultraviolet absorption spectra. The absorption intensity of characteristic peaks increase with a four-layer cycle, indicating that the LBL assembly film grow linearly and reproducibly from layer to layer. The composition of the film was measured by X-ray photoelectron spectrum (XPS). The data of XPS confirmed the presence of the expected elements. The film exhibited photoluminescence arising from $\pi^* - t_{2g}$ ligand-to-metal transition of Ru(bpy) and redox activity attributing to molybdenum-centered redox processes of PMo_{12}. The surface morphology of multilayer film was characterized by atomic force microscopy (AFM). The result shows that the film had a smooth surface with root-mean-square (rms) roughness ca. 1.363 nm for $\{PEI/(PSS/PEI/PMo_{12}/Ru(bpy))_3\}$. The grains are homogeneously dispersed in the substrate and have a rather narrow diameter size distribution.

Keywords: Layer-by-layer self-assembly; Polyoxometalate; Luminescence; Film; Ruthenium

1. Introduction

Polyoxometalates (POMs) have been the subject of many areas of materials science due to their potential applications in catalysis, conductivity, photo- and electrochromic devices, and molecular electronics [1–3]. Particular attention has been given to POMs-based functional materials and devices [4–10]. The method of layer-by-layer (LBL) self-assembly provides a powerful tool for the formation and development of POM-based films in that it is a simple yet effective technique to prepare uniform multilayer films, based just on alternate adsorption of oppositely charged polyelelctrolytes or polyions by electrostatic attractions between them [11–16]. Inorganic and organic components can be assembled orderly into multilayer films by this way to provide a high degree of control over composition, thickness, and orientation of each layer on the level of molecule, which offer potential advantages for thin film materials in molecular electronic devices [17–21]. By using the LBL method, Ichinose et al. fabricated thin film based on iso-polymolybdate $[Mo_8O_{26}]^{4-}$ and poly(allylamine hydrochloride), and Moriguchi et al. fabricated electrochromic film based on decatungstate $[W_{10}O_{32}]^{4-}$ and poly(diallyldimethylammonium chloride) [5,22]. Kurth group has obtained many achievements on the incorporation of POMs into LBL thin films recently, such as $[H_3Mo_{57}V_6(NO)_6O_{183}(H_2O)_{18}]^{21-}$, $[Mo_{132}O_{372}(CH_3COO)_{30}(H_2O)_{27}]^{42-}$, $[Co_4(H_2O)_2P_4W_{30}O_{112}]^{16-}$, $[Eu\text{-}(H_2O)P_5W_{30}O_{110}]^{12-}$ and $[Na(H_2O)P_5W_{30}O_{110}]^{14-}$ [8, 23–26]. Our group has done much work in this field too [9,10,27].

Transition metal complexes, such as tris(2,2-bipyridine) ruthenium $[Ru(bpy)_3]^{2+}$, have been the subject of extensive electrochemical and spectroscopic studies, due to their excellent photoluminescence properties and excellent stability in multiple redox states. Electronic

*Corresponding author. Fax: +86-431-568-4009.
E-mail address: jpeng@nenu.edu.cn (J. Peng).

0022-4596/$ - see front matter © 2004 Published by Elsevier Inc.
doi:10.1016/j.jssc.2004.05.054

carriers can be readily injected and transported in these transition metal complexes, which make them promising candidates for electroluminescent devices [28]. Handy et al. demonstrated that high efficiency devices could be fabricated by a single-layer, spin-coated film of a low molecular weight ruthenium complex, which $[Ru(bpy)_3]^{2+}(PF_6^-)_2$ is a model compound for this class of materials [29]. In order to explore the potential application of transition metal complexes in the design and construction of molecular electronic devices, it is important to design, fabricate, and study functional films containing transition metal complexes.

However, relatively little are reported about the combining POMs with tris(2,2-bipyridine) ruthenium [30–33]. So in this paper, we described the fabrication of a nanocomposite ultrathin film based on PMo_{12} and Ru(bpy) by using the LBL method. The growth of {PEI/(PSS/PEI/PMo_{12}/Ru(bpy))$_n$} film was monitored by ultraviolet-visible absorption spectra and the film structure was observed by atomic force microscopy (AFM). The photoluminescent properties of the film were examined by fluorescence spectroscopy. Electrochemistry property of the film was also investigated.

2. Experimental section

2.1. Materials and instruments

Poly(ethylenimine) (PEI; MW. 750,000) and poly (styrenesulfonate) (PSS; MW. 70.000), were commercially obtained from Aldrich and used without further purification. Polyoxometalate $H_3PMo_{12}O_{40}$ was purchased from Beijing Chem. Corp. of China and used without further purification. The $[Ru(bpy)_3]Cl_2$ was prepared by the literature [34]. The water used in all experiments was deionized to a resistivity of 16–18 MΩ cm. All other reagents were of reagent grade.

UV–vis spectra were recorded on a 756 CRT UV-vis spectrophotometer made in Shanghai, China. X-ray photoelectron spectra (XPS) were performed on an Escalab MKII photoelectronic spectrometer with Mg$K\alpha$ (1253.6 eV) as X-ray source. AFM images were obtained by using digital nanoscope IIIa instrument operating in the tapping mode with silicon nitride tips. Fluorescence spectra were performed with a SPEX FL-2T2 fluorescence spectrophotometer using a 450 W xenon lamp as excitation source. A CHI 600 electrochemical workstation connected to digital-586 personal computer was used for control of the electrochemical measurements and for data collection. A conventional three-electrode system was used, with a {PEI/(PSS/PEI/PMo_{12}/Ru(bpy))$_n$} multilayer film coated ITO electrode as a working electrode, platinum foil as a counter electrode, and Ag/AgCl as a reference electrode, in pH 4.0 buffer solutions.

2.2. LBL assembly

The fabrication of the multilayer film was carried out as follows. The substrate (silica or quartz glass slide) was cleaned according to the literature [23], which made its surface become hydrophilic, rinsed with deionized water, dried under a nitrogen stream. The hydrophilized substrate slide was immersed in 3×10^{-2} mol L^{-1} PEI solution (the concentration was calculated based on their repeating units) for 20 min, followed by washing with deionized water. After washing, a nitrogen stream was blown over the film surface until the adhering water layer was completely removed. The PEI-coated substrates then were alternately dipped into 1×10^{-2} mol L^{-1} PSS, 1×10^{-2} mol L^{-1} PEI, 1×10^{-3} mol L^{-1} PMo_{12} and 1×10^{-2} mol L^{-1} Ru(bpy) for 20 min, also rinsed with deionized water, and dried in a nitrogen stream after each dipping. Multilayer film {PEI/(PSS/PEI/PMo_{12}/Ru(bpy))$_n$} (schematic representation shown in Fig. 1) were formed in matrix.

ITO glass (on one side only) substrate was cleaned by immersing into a H_2SO_4:H_2O_2 = 7:3 (V/V) solution for a few minutes followed by rinsing copiously with deionized water and drying in a nitrogen stream [22]. LBL deposition was performed according to the process as described above.

3. Results and discussion

3.1. Ultraviolet-visible absorption spectra

The formation of the multylayer film was monitored by the UV spectroscopy. The absorbencies of per

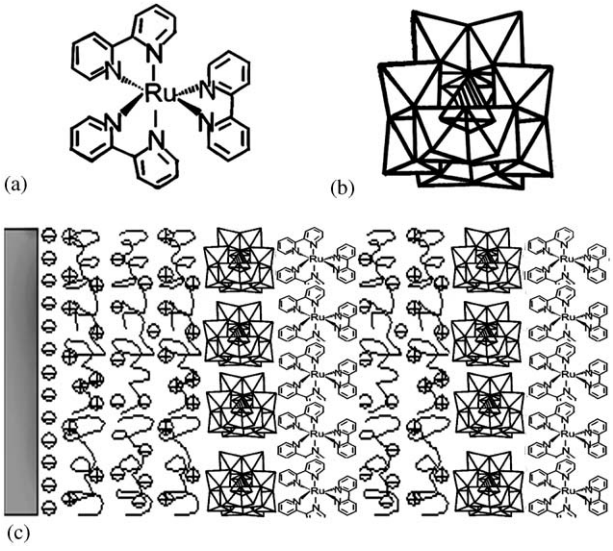

Fig. 1. The structure of (a) Ru(bpy) and (b) PMo_{12}; (c) schematic illustration of the {PEI/(PSS/PEI/PMo_{12}/Ru(bpy))$_n$} multilayer film, $n = 2$.

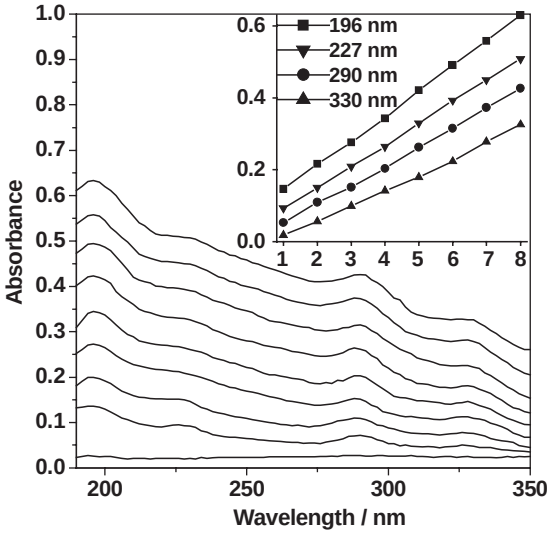

Fig. 2. UV absorption spectra of multilayer film of {PEI/(PSS/PEI/PMo_{12}/Ru(bpy))$_n$} (from bottom to top, $n = 0$, 1, 2, 3, 4, 5, 6, 7, and 8) assembled on a quartz substrate (on both sides). The inset shows plots of the absorbance values at 196, 227, 290, and 330 nm as a function of the number of the PSS/PEI/PMo_{12}/Ru(bpy) four-layer cycle.

four-layer cycle were obtained for film assembled on two sides of a quartz slide. Fig. 2 exhibits the UV spectra of {PEI/(PSS/PEI/PMo_{12}/Ru(bpy))$_8$} multilayer film deposited on a quartz slide in 190–350 nm. The spectra showed four peaks at 196, 227, 290, and 330 nm, respectively. As is reported, over our investigated wavelength range, Ru(bpy) has three characteristic absorptions, ligand-centred $\pi-\pi^*$ transition at 299 nm, and metal-centred $d-d$ transitions at 237 and 327 nm [30,35]; PMo_{12} has two characteristic absorptions, $O_d \rightarrow W$ at 212 nm and $O_b(O_c) \rightarrow W$ at 310 nm (O_d = terminal oxygen, O_b and O_c = bridge oxygen) [36]; PSS has two characteristic absorptions of pendent aromatic groups at 195 and 225 nm [37]. So the absorption at 196 nm can be assigned to the overlap peak of PMo_{12} and PSS; the absorption at 227 nm can be assigned to the overlap peak of PSS and Ru(bpy); the absorption at 290 nm can be assigned to Ru(bpy); the absorption at 330 nm can be assigned to the overlap peak of Ru(bpy) and PMo_{12}. The absorbencies of these peaks increased linearly with the number of deposition cycle (see Fig. 2 inset), suggesting that the quantity of these species deposited per cycle was constant up to at least an n value of 8.

3.2. Atomic force microscopy

Topographical characterization was conducted by AFM. Fig. 3a and b show the AFM images corresponding to the {PEI/(PSS/PEI/PMo_{12}/Ru(bpy))$_2$ (PSS/PEI/PMo_{12})} and {PEI/(PSS/PEI/PMo_{12}/Ru(bpy))$_3$}, respectively. The layer of PMo_{12} onto the {PEI/(PSS/PEI/PMo_{12}/Ru(bpy))$_2$ (PSS/PEI/)} shows a relatively uniform and smooth surface with a rms roughness of

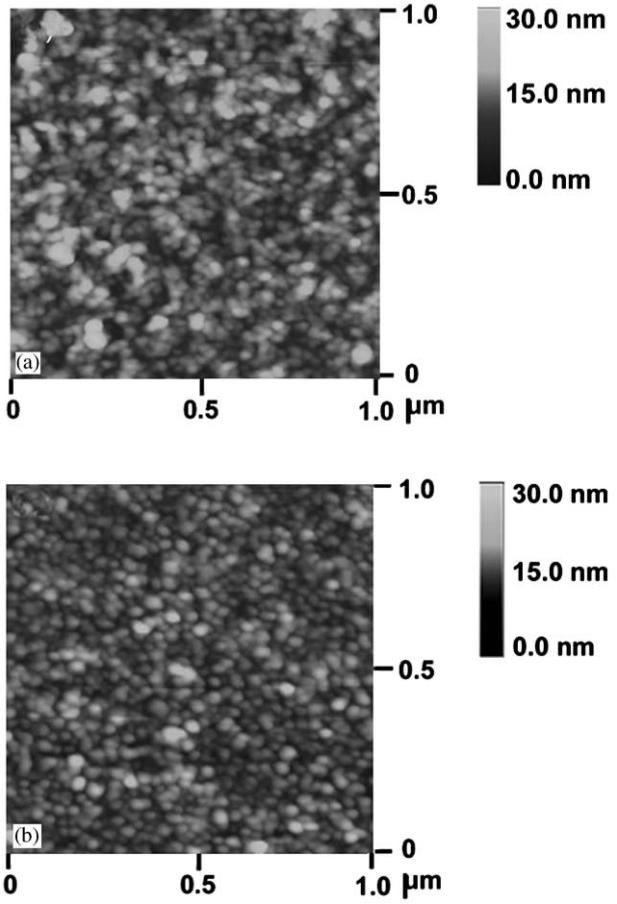

Fig. 3. AFM images of (a) {PEI/(PSS/PEI/PMo_{12}/Ru(bpy))$_2$ (PSS/PEI/PMo_{12})} and (b) {PEI/(PSS/PEI/PMo_{12}/Ru(bpy))$_3$} multilayer films.

2.959 nm, on which the PMo_{12} nanoparticles with a mean grain size of ca. 40 nm aggregate into nanoclusters. However, when an Ru(bpy) layer was deposited on the top of the {PEI/(PSS/PEI/PMo_{12}/Ru(bpy))$_2$(PSS/PEI/PMo_{12}/)}, the film showed a significantly different surface morphology compared with the former PMo_{12} layer. The Ru(bpy) layer shows much smoother surface with smaller rms roughness 1.363 nm, on which the aggregate degree of grains decreases largely. The significant difference of surface morphology between the two layers is possibly because that the cationic polymer PEI reduced the coulombic repulsion of adjacent PMo_{12} centers, leading to aggregating of PMo_{12} to a certain extent [22,38].

3.3. Luminescent property

The excitation spectra of the Ru(bpy) solid and {PEI/(PSS/PEI/PMo_{12}/Ru(bpy))$_{10}$} LBL film self-assembled on smooth quartz substrate at room temperature were showed in Fig. 4. As can be seen from Fig. 4, the two spectra are similar and both have the most intense bands at ca. 470 nm assigned to the singlet metal-to-ligand

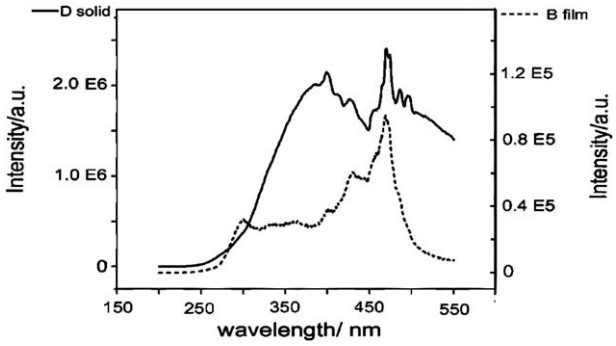

Fig. 4. Excitation spectra of solid Ru(bpy) (D) and {PEI/(PSS/PEI/PMo_{12}/Ru(bpy))$_{10}$} multilayer film (B).

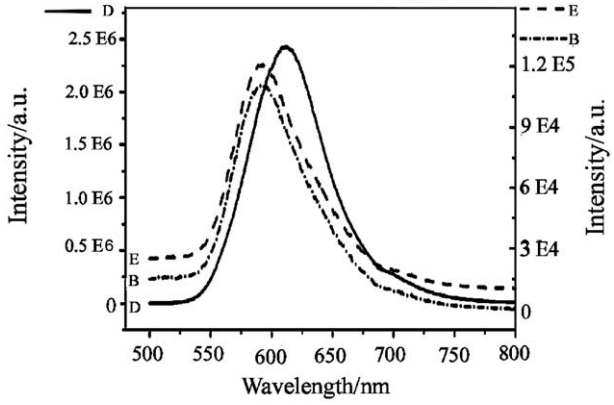

Fig. 5. Emission spectra of solid Ru(bpy) (D) and {PEI/(PSS/PEI/PMo_{12}/Ru(bpy))$_n$} multilayer films (B and E, $n = 10$ and 12).

(MLCT) $d-\pi^*$ transitions [28], while certain variations occured in the band number, band position, and relative intensity of some individual bands in the spectrum of the film. Particularly, in contrast to the spectrum of Ru(bpy) solid, the intensity of the broad band centered at 398 nm decreases greatly, and the much less intense bands at 486 and 498 nm disappear in the film. The emission spectra of the Ru(bpy) solid and {PEI/(PSS/PEI/PMo_{12}/Ru(bpy))$_n$} ($n = 10$ and 12) LBL films are showed in Fig. 5, excited at 470 nm. The emission spectra for Ru(bpy) solid and the thin films are quite similar and all show a characteristic broad band, arising from $\pi^* - t_{2g}$ ligand-to-metal transition of Ru(bpy) [28]. The luminescence bands are, however, blue-shifted from 612 to 592 nm in thin films. All these changes as mentioned above may be associated with the strong interactions between tris(2,2-bipyridine) ruthenium and the polyanion, and the polyelectrolyte, which have influence on the molecular orbitals of ligands and metal in Ru(bpy). The blue-shifted phenomenon is also observed in previously reported Ru(bpy) [39–41]. The luminescence intensity of thin films increased with the number of deposition cycle, and the band positions are found remain invariant, suggesting that the films were made uniformly. The electroluminescence behavior of the multilayer film is underway.

3.4. X-ray photoelectron spectrum

XPS measurements were performed to identify elemental composition of {PEI/(PSS/PEI/PMo_{12}/Ru(bpy))$_3$} LBL film deposited on the single-crystal silicon substrate. The film exhibited peaks corresponding to C1*s* (BE = 285.0 eV), N1*s* (BE = 401.8 eV and BE = 399.5 eV), O1*s* (BE = 531.3 eV), P2*p* (BE = 133.1 eV), S2*p* (BE = 168.1 eV), Mo3*d* 5/2 (BE = 232.4 eV), and Mo3*d* 3/2(BE = 235.1 eV), whereas that for Ru was not observed due to its very low percentages in the film (detection limit required by the instrument is $\geqslant 2\%$). The C1*s* signal can be assigned to the carbon in PEI and PSS; the O1*s* is ascribed to the oxygen atoms in PSS and PMo_{12}. The appearance of double N1*s* peaks at 401.8 and 399.5 eV in the XPS measurement indicates that there are two kinds of nitrogen atoms in the thin film (see Fig. 6). One kind of nitrogen atom comes from polyelectrolyte PEI, corresponding to the N1*s* peak at 401.8 eV. The other kind is attributed to the nitrogen atom of the N–Ru coordination bond in Ru(bpy), corresponding to the N1*s* peak at 399.5 eV. These XPS results confirm the existence of the polyelectrolytes, PMo_{12}, and Ru(bpy) in the multilayer film in conjunction with the results of UV-vis and fluorescent spectra.

3.5. Electrochemistry of the {PEI/(PSS/PEI/PMo_{12}/Ru(bpy))$_{12}$} film self-assembled on ITO glass substrate

Polyoxometerlates have good redox activity and are extensively used as the electrocatalysts, so the electrochemical method can be chosen to characterize the

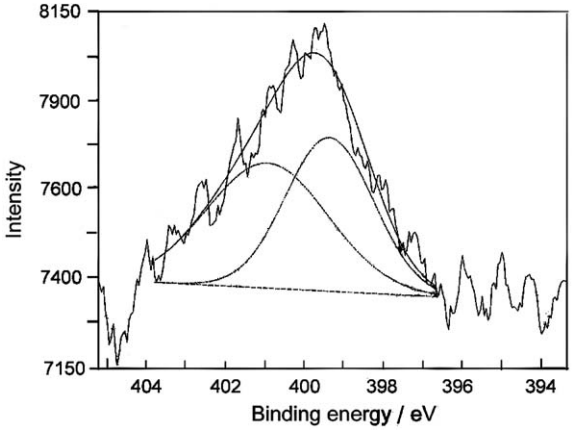

Fig. 6. XPS spectrum of N1*s* in the {PEI/(PSS/PEI/PMo_{12}/Ru(bpy))$_n$} multilayer film.

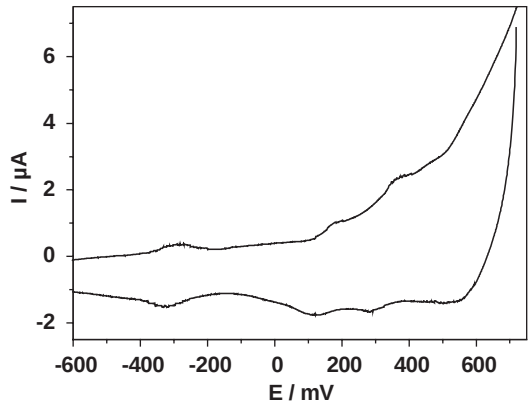

Fig. 7. Cyclic voltammogram of {PEI/(PSS/PEI/PMo_{12}/Ru(bpy))$_{12}$} multilayer film on ITO electrode in 0.1 M blank Na_2SO_4. Scan rate: 5 mV s^{-1}.

property of film based on them. The CV of the {PEI/(PSS/PEI/PMo_{12}/Ru(bpy))$_{12}$}-modified ITO electrode in 0.2 M Na_2SO_4 solution (pH = 4) was exhibited in Fig. 7. In the range −600 and 800 mV, the thin film undergo three redox waves with the surface formal potential $E^{o'}_{sur}$ values of 325, 192, and −305 mV, respectively, which should be assigned to molybdenum-centered redox processes of PMo_{12} [42]. The result suggested that the electrochemical property of PMo_{12} is being maintained in the LBL film.

4. Conclusion

The well-behaved multilayer film based on Keggin-type polyoxometalate $PMo_{12}O_{40}^{3-}$ and transition metal complex tris(2,2-bipyridine) ruthenium $[Ru(bpy)_3]^{2+}$ was prepared by using LBL assembly and characterized by UV-vis spectra, XPS, and AFM images. The film exhibited photoluminescence arising from $\pi^* - t_{2g}$ ligand-to-metal transition of Ru(bpy) and good redox activity attributing to molybdenum-centered redox processes of PMo_{12}. The results provide an implication that a series of luminescence multilayer films may be fabricated by incorporating POMs with transition metal complexes, which would represent potential applications in organic light emitting devices and electrocatalysis.

Acknowledgments

This work was supported by the National Nature Science Foundation of China (20271001) and the Nature Science Foundation of Heilongjiang Province in China (B0308).

References

[1] C.L. Hill, Chem. Rev. 98 (1998) 1.
[2] M.T. Pope, A. Muller, Polyoxometalates: From Platonic Solid to Anti-retroviral Activity, Kluwer, Dordrecht, 1994.
[3] T. Yamase, Chem. Rev. 8 (1998) 307.
[4] A. Kuhn, F.C. Anson, Langmuir 12 (1996) 5481.
[5] I. Ichinose, H. Tagawa, S. Mizuki, Y. Lvov, T. Kunitake, Langmuir 14 (1998) 187.
[6] M. Clemente-Leon, B. Agricole, C. Mingotand, C.J. Gomez-Garcia, E. Coronado, P. Delhaes, Angew. Chem. Int. Ed. Engl. 36 (1997) 1114.
[7] L. Cheng, S.J. Dong, J. Electrochem. Soc. 147 (2000) 606.
[8] S.Q. Liu, D.G. Kurth, H. Möhwald, D. Volkmer, Adv. Mater. 3 (2002) 225.
[9] L. Xu, H.Y. Zhang, E.B. Wang, D.G. Kurth, Z. Li, J. Mater. Chem. 12 (2002) 654.
[10] M. Jiang, E.B. Wang, G. Wei, L. Xu, Z.H. Kang, Z. Li, New J. Chem. 27 (2003) 1291.
[11] T. Katsuno, S. Nitta, K. Ueda, J. Non-Cryst. Solids 299 (2002) 830.
[12] M.R. Linford, M. Auch, H. Möhwald, J. Am. Chem. Soc. 120 (1998) 178.
[13] J.H. Fendler, F.C. Meldrum, Adv. Mater. 7 (1995) 607.
[14] N.A. Kotov, F.C. Meldrum, J.H. Fendler, J. Phys. Chem. 98 (1994) 8827.
[15] S.W. Keller, H.N. Kim, T.E. Mallouk, J. Am. Chem. Soc. 116 (1994) 8817.
[16] H.N. Kim, S.W. Keller, T.E. Mallouk, J. Smitt, G. Decher, Chem. Mater. 9 (1997) 1414.
[17] G. Tovar, S. Paul, W. Knoll, O. Prucker, J. Ruhe, Supramol. Sci. 2 (1995) 89.
[18] D. Piscevic, W. Knoll, M.J. Tarlov, Supramol. Sci. 2 (1995) 99.
[19] H.E. Katz, G. Sheller, T.M. Putvinski, M.L. Shilling, W.L. Wilson, CED Chidsey Sci. 254 (1991) 1485.
[20] M. Ferreira, J.H. Cheung, M.F. Rubner, Thin Solid Films 244 (1994) 806.
[21] A.C. Fou, O. Onisuka, M. Ferreira, M.F. Rubner, J. Appl. Phys. 79 (1996) 7501.
[22] I. Moriguchi, J.H. Fendler, Chem. Mater. 10 (1998) 2205.
[23] F. Caruso, D.G. Kurth, D. Volkmer, M.J. Koop, A. Muller, Langmuir 14 (1998) 3462.
[24] D.G. Kurth, D. Volkmer, Chem. Mater. 12 (2000) 2829.
[25] S.Q. Liu, D.G. Kurth, D. Volkmer, Chem. Commun. (2002) 976
[26] S.Q. Liu, D.G. Kurth, B. BredenkÖtter, D. Volkmer, J. Am. Chem. Soc. 124 (2002) 12280.
[27] H.Y. Ma, J. Peng, Z.G. Han, Y.H. Feng, E.B. Wang, Thin Solid Film 446 (2003) 161.
[28] J. Slinker, D. Bernards, P.L. Houston, H.D. Abruña, S. Bernhard, G.G. Malliaras, Chem. Commun. (2003) 2392.
[29] E.S. Handy, A.J. Pal, M.F. Rubner, J. Am. Chem. Soc. 121 (1999) 3525.
[30] N. Fay, E. Dempsey, A. Kennedy, T. McCormac, J Electroanal. Chem. 556 (2003) 63.
[31] A. Kuhn, F.C. Anson, Langmuir 12 (1996) 5481.
[32] V.M. Hultgren, A.M. Bond, A.G. Weld, J. Chem. Soc., Dalton Trans. (2001) 1076.
[33] Z. Han, E. Wang, G. Luan, Y. Li, C. Hu, P. Wang, N. Hu, H. Jia, Inorg. Chem. Commun. 4 (2001) 427.
[34] I. Fujita, H. Kobayashi, Ber. Bunsen-Ges, Phys. Chem. 76 (1972) 115.
[35] J.E. Fergusson, G.M. Harris, J. Chem. Soc. (A) (1966) 1293.
[36] L. Xu, E.B. Wang, Z. Li, D.G. Kurth, X.G. Du, H.Y. Zhang, C. Qin, New J. Chem. 26 (2002) 782.

[37] M.R. Linford, M. Auch, H. Mõhwald, J. Am. Chem. Soc. 120 (1998) 178.
[38] Y.H. Wang, C.X. Guo, Y.W. Chen, C.W. Hu, W.H. Yu, J. Colloid Interface Sci. 264 (2003) 176.
[39] J.N. Demas, G.A. Crosby, J. Am. Chem. Soc. 93 (1971) 2841.
[40] M. Ogawa, T. Nakamura, J.I. Mori, K. Kuroda, J. Phys. Chem. B 104 (2000) 8554.
[41] J. Wheeler, J.K. Thomas, J. Phys. Chem. 86 (1982) 4540.
[42] S. Dong, Z. Jin, J. Chem. Soc. Chem. Commun. (1987) 1871.